Geol. Mag. **145** (*1*), *2008, pp. 1–15.* © *2007 Cambridge University Press*
doi:10.1017/S0016756807003949 First published online 5 October 2007 *Printed in the United Kingdom*

The Miocene igneous rocks in the Basal Unit of Lavrion (SE Attica, Greece): petrology and geodynamic implications

NIKOS SKARPELIS*, BASILIOS TSIKOURAS† & GEORGIA PE-PIPER‡

*Department of Geology & Geoenvironment, University of Athens, Panepistimiopoli, 157 84 Zografou, Athens, Greece
†Department of Geology, Section of Earth Materials, University of Patras, 265 00 Patras, Greece
‡Department of Geology, Saint Mary's University, Halifax, NS B3H 3C3, Canada

(*Received* 24 October 2006; *accepted* 2 April 2007)

Abstract – The Miocene igneous rocks in the Basal Unit of the Lavrion area form part of the granitoid province of the central Aegean. Undeformed, subvertical dykes of quartz-syenite to granodiorite and granite porphyries, and a little deformed but variably altered granodiorite stock intrude metamorphic rocks of the Basal Unit. A 9.4 ± 0.3 Ma K–Ar age on feldspar for a dyke rock provides a minimum age for the igneous activity in the Basal Unit. East–west orientation of porphyry dykes is indicative of a regional extensional stress field with roughly north–south direction. Substantial extension in the Basal Unit after granodiorite emplacement is evident from widespread quartz veining associated with hydrothermal alteration of the granodiorite and the occurrence of mineralized tension gashes cutting the hydrothermally altered hornfelses. Final emplacement of the Blueschist Unit over the Basal Unit by extensional detachment post-dates contact metamorphism of the rocks surrounding the granodiorite. Geochemical diagrams show a continuous range of compositions from the dykes to the granodiorite. Radiogenic isotope compositions are compatible with a common magmatic source for the two lithologies. Elemental variations, as well as the considerable geochemical similarity of the dyke rocks to the Hercynian paragneiss of the central Cyclades, indicate that crustal melts were significant components during the evolution of the igneous rocks with fractional crystallization as an important process during later stages of evolution. The granodiorite displays geochemical signatures indicative of a significant mafic mantle-derived magma component.

Keywords: granodiorite, dykes, Miocene, extensional tectonics, Lavrion, Greece.

1. Introduction

The SE part of Attica (Greece) (Fig. 1), known also as the 'Lavrion area' or the 'Lavreotiki peninsula', has been famous for mining and processing of argentiferous ore since the 10th century BC and for the production of silver and lead contributing to the economic development of ancient Athens during the classic era. Lavrion has attracted the interest of mineral collectors and has become a site of great importance for studies in the fields of industrial archaeology and the environmental impact of old mining and metallurgical activities. The geology and metallogeny of Lavrion were studied by Marinos & Petrascheck (1956). During the following years only a little geological work was carried out in the area on structures and petrology of regionally metamorphosed rocks and on the igneous rocks (Kessel, 1990; Papanikolaou & Syskakis, 1991; Baltatzis, 1996; Altherr & Siebel, 2002), in comparison to the neighbouring Cycladic islands, which have been extensively studied. These igneous rocks in SE Attica are the most westerly occurrence of a series of Middle to Late Miocene plutons and hypabyssal rocks in the Attic–Cycladic belt that were emplaced following the peak of Barrovian metamorphism during widespread extension and mid-crustal detachment (Buick, 1991; Gautier & Brun, 1994). The aim of this paper is to present new data on the geology, age and petrology of the igneous rocks occurring in the Basal Unit, in an attempt to interpret the geodynamic setting of these Late Miocene intrusive rocks of the area.

*Author for correspondence: skarpelis@geol.uoa.gr

2. Regional setting

The area of Lavrion forms part of the Attic–Cycladic belt (Fig. 1), which belongs to the central Hellenides and is composed of a stacked sequence of nappes mainly emplaced in the Early Eocene (Dürr *et al.* 1978). In the Attic–Cycladic belt four major tectonostratigraphic units can be distinguished:

(a) The Basal Unit (para-autochthon) represents a remnant of a carbonate platform of Late Triassic to Late Cretaceous age, overlain by Tertiary anchimetamorphic flysch (e.g. Dubois & Bignot, 1979; Minoux, Bonneau & Kienast, 1980; Avigad & Garfunkel, 1989). Glaucophane relics and Si-rich phengites in the metaflysch indicate that the para-autochthon underwent high-pressure/low-temperature metamorphism (Shaked, Avigad & Garfunkel, 2000). Rb–Sr dating on high-Si-phengite from mica-rich

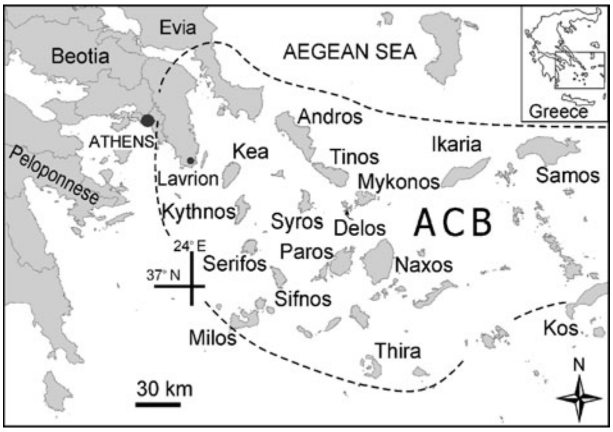

Figure 1. Geographic map of the south Aegean region indicating the extent of the Attic–Cycladic Belt (ACB) and locations discussed in the text.

metapelites yielded ages of *c.* 23 Ma (Ring & Reischmann, 2002). These dates along with similar Rb–Sr dates on high-Si-phengite from the Basal Unit on Tinos (Bröcker & Franz, 1998) and $^{40}Ar/^{39}Ar$ dates from Samos (Ring, Layer & Reischmann, 2001) were interpreted by Ring & Reischmann (2002) as the age of the high-pressure metamorphism. Bröcker *et al.* (2004) instead suggested that this age constrains the timing of the greenschist-facies overprint.

(b) The Lower Unit, dominating in the central Aegean, comprises mainly Carboniferous basement orthogneisses and post-Carboniferous volcano-sedimentary sequences of interbedded metabasites, marbles and metapelites affected by eclogite- to blueschist-facies metamorphism during the Eocene (e.g. Altherr *et al.* 1979; Okrusch & Bröcker, 1990; Trotet, Vidal & Jolivet, 2001). Cretaceous zircon SHRIMP $^{206}Pb–^{238}U$ ages from an eclogite (S. Keay, unpub. Ph.D. thesis, Australian National Univ. 1998) and similar results from meta-igneous lithologies from Syros (Tomaschek *et al.* 2003) were related to the presence of an inherited magmatic component, whereas zircon rims yielding Eocene ages were interpreted to date high-pressure metamorphism. Cretaceous U–Pb ages of zircons from high-pressure rocks from Tinos and Syros reported by Bröcker & Enders (1999) and Bröcker & Keasling (2006) were interpreted as reflecting hydrothermal or metasomatic processes in a subduction zone environment, indicating that the Cycladic blueschist belt recorded both Cretaceous and Eocene high-pressure episodes.

The high-pressure metamorphic event was a consequence of Alpine orogenesis during Cretaceous to Eocene subduction of the Apulian microplate beneath Eurasia (Dürr *et al.* 1978). High-pressure rocks were partly overprinted by Miocene (25–16 Ma) greenschist- to amphibolite-facies metamorphism during exhumation (e.g. Altherr *et al.* 1982; Bröcker *et al.* 1993; Avigad *et al.* 1997; Parra, Vidal & Jolivet, 2002). In the southern Cyclades (Naxos, Paros), the overprint culminated in anatectic processes (e.g. Altherr *et al.* 1979, 1982; Wijbrans & McDougall, 1988).

(c) The Upper Unit, which tectonically overlies the Lower Unit, consists of both non-metamorphic Late Permian to Middle Triassic volcaniclastic rocks, Late Triassic–Jurassic carbonate rocks and remnants of Eo-Hellenic ophiolites transgressively covered by Late Cretaceous carbonates, and various sequences of Late Cretaceous high-temperature/low-pressure metamorphic rocks (e.g. Reinecke *et al.* 1982; Papanikolaou, 1987; Altherr *et al.* 1994). The HT–LP metamorphic rocks comprise mainly orthogneisses, amphibolites and a dismembered ophiolite (Katzir *et al.* 1996).

(d) Early to Late Miocene shallow marine to continental sediments overlie the Cycladic Blueschist Unit or the ductile shear zones of granitoids (Dermitzakis & Papanikolaou, 1980; Böger, 1983; Dürr & Altherr, 1979; Sánchez-Gómez, Avigad & Heimann, 2002). They were deposited in half-graben basins formed during the Aegean back-arc extension (Gautier & Brun, 1994).

Late orogenic extension overprinted the stacked nappes. Studies on metamorphic core-complexes in the Cyclades have suggested that back-arc extension began at least in Early Miocene times, when the Eocene eclogites and blueschist rocks underwent the greenschist- to amphibolite-facies metamorphism. Large-scale extension in the Aegean was achieved by low-angle normal faults, which caused exhumation of ductile basement rocks to surface levels (e.g. Lister, Banga & Feenstra, 1984; Gautier & Brun, 1994; Avigad *et al.* 1997; Jolivet *et al.* 2003; Ring & Layer, 2003).

Miocene extension in the Attic–Cycladic belt was accompanied by the emplacement of I- and S-type granitoid magmas. Numerous granitoids intruded the Cycladic realm between 15 and 9 Ma (Altherr *et al.* 1982; Skarpelis, Kyriakopoulos & Villa, 1992; Pe-Piper, Piper & Matarangas, 2002) and in places caused contact metamorphism of the surrounding rocks and development of skarns and skarn-type mineralization (Salemink, 1985; Skarpelis & Liati, 1990; Bröcker & Franz, 1994). Emplacement of the numerous plutons in the Cycladic metamorphic complex was synchronous with extensional detachment faulting (e.g. Lister, Banga & Feenstra, 1984; Buick, 1991). Magma locally pierced the detachments and/or suffered syn-extensional shearing (Altherr *et al.* 1982; Faure, Bonneau & Pons, 1991; Lee & Lister, 1992). Most Miocene plutons of the central Aegean are classified as I type. Monzonitic to monzogranitic intrusive rocks are exposed in the ENE (Kos, Samos), granites in the centre and south (Tinos, Mykonos, Naxos, Delos, Ikaria, Thera) and granodiorites in the WNW (Serifos, Lavrion) (Altherr *et al.* 1988; Altherr & Siebel, 2002). The present South Aegean Volcanic Arc is located to the southern part of the Cyclades and mimics the southward retreat of the subduction zone.

https://doi.org/10.1017/S0016756807003949 Published online by Cambridge University Press

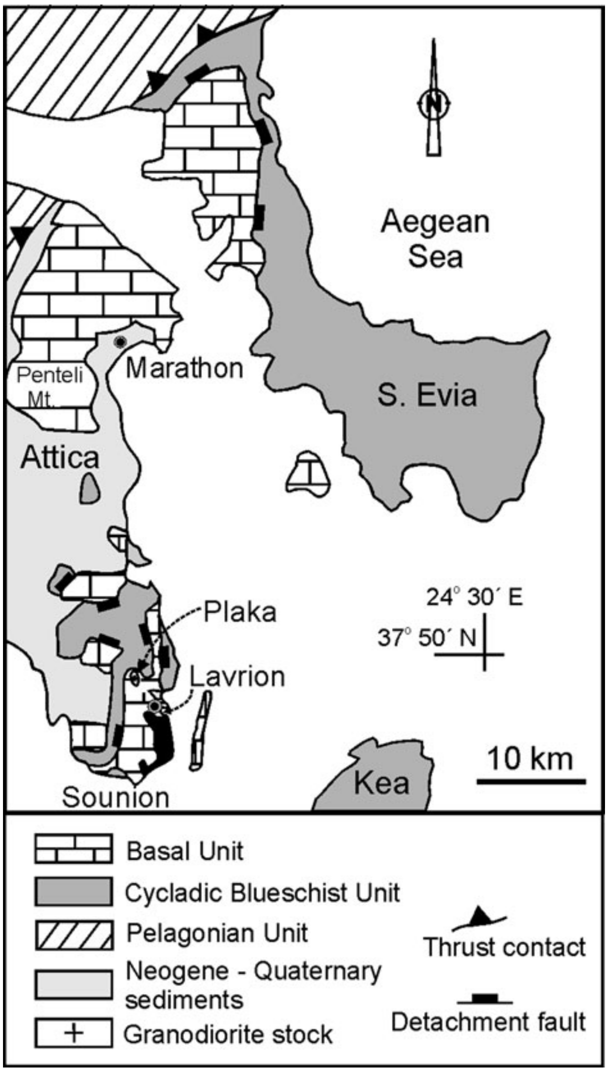

Figure 2. Simplified geological map of eastern Attica and south Evia island (modified after Marinos & Petrascheck, 1956; Katsikatsos *et al.* 1986 and Shaked, Avigad & Garfunkel, 2000).

3. Geology of Lavrion area

In the Lavrion area, the tectonostratigraphy consists of two units: the 'Basal Unit' (para-autochthon) and the 'Blueschist Unit' (allochthon), which is a part of the Cycladic Blueschist Unit. A detachment fault separates the Basal from the Blueschist Unit (Figs 2, 3, 4). The original contact between the two units was a thrust plane (Marinos & Petrascheck, 1956; Kessel, 1990), developed during the Eocene or Oligocene compression of the Cyclades. The Basal Unit comprises metaclastic rocks with intercalations of carbonates ('Kaesariani schists') sandwiched between mylonitized marbles ('Upper' and 'Lower' marbles). Fossils within the 'Basal Unit' indicate a Late Triassic–Early Jurassic age (Marinos & Petrascheck, 1956). Elsewhere in Attica and in southern Evia, the para-autochthon (referred to as 'Almyropotamos–Attica Unit' by Katsikatsos *et al.* 1986) is composed mainly of a thick sequence of Triassic–Jurassic to Late Cretaceous marbles with schist intercalations (Marinos & Petrascheck, 1956; Katsikatsos, 1977). Occurrence of high-Si phengite in metapelites from Attica indicates that they underwent a high-pressure metamorphism (Baziotis, Mposkos & Perdikatsis, 2006). Metamorphosed igneous rocks, bearing high-silica phengite, occur within the metaclastic subunit of the 'Basal Unit' in the Lavrion area. An Early Miocene age can be assumed for the regional metamorphism of the 'Basal Unit' at Lavrion by analogy with dated rocks in the 'Almyropotamos Unit' in south Evia (Ring & Reischmann, 2002; Ring & Layer, 2003).

The 'Blueschist Unit' comprises high-pressure/low-temperature metapelites, metasandstones, marbles, metabasic rocks and minor quartzite. Sills of hydrothermally altered S-type porphyritic granitoid rock occur within metapelites along or close to the detachment fault. Research on the petrology of these rocks is in progress. An Eocene age for the peak of the high-pressure/low-temperature metamorphism was postulated (Altherr *et al.* 1982; Ring & Layer, 2003). The mineralogy, petrochemistry and *P–T* path of the metabasic rocks were studied by Baltatzis (1996). He concluded that they had experienced a progressive transformation of possibly eclogite-facies rocks through epidote blueschists into greenschists. Late Cretaceous limestones (Leleu & Neumann, 1969) tectonically overlie the Blueschist Unit and are possibly equivalent to Late Cretaceous carbonates of the Upper Cycladic Unit.

Middle Miocene sediments, tectonically overlying the Blueschist Unit, comprise lacustrine and brackish deposits (Marinos & Petrascheck, 1956).

4. Geological setting of the granitoid rocks

4.a. The granodiorite stock

An almost undeformed but variably altered granodiorite stock crops out in the Plaka area (Fig. 3), intruding the 'Basal Unit'. The granodioritic stock is considered to be an apophysis of a granitic batholith, existing at depth in the eastern part of Attica, detected by geophysical measurements (Marinos & Makris, 1975). A weak pre-full-crystallization subhorizontal mineral fabric is observed. An age of 8.27 ± 0.11 Ma by K–Ar on biotite was reported by Altherr *et al.* (1982), whereas Marinos (1971) obtained a K–Ar whole rock age of 8.8 ± 0.5 Ma. It is worth mentioning that elsewhere in the Cyclades, K–Ar and ^{39}Ar–^{40}Ar biotite ages are typically several million years younger than hornblende ages (Altherr *et al.* 1982), even in relatively high-level stocks such as in Samos (Mezger *et al.* 1985; Pe-Piper & Piper, 2004). A fission track age of 7.3 Ma on apatite (G. Wagner *in* Altherr *et al.* 1982) indicates rapid cooling of the plutonite. Intrusion of the granodiorite was accompanied by contact metamorphism of the surrounding 'Kaesariani schists' (Baltatzis, 1981).

https://doi.org/10.1017/S0016756807003949 Published online by Cambridge University Press

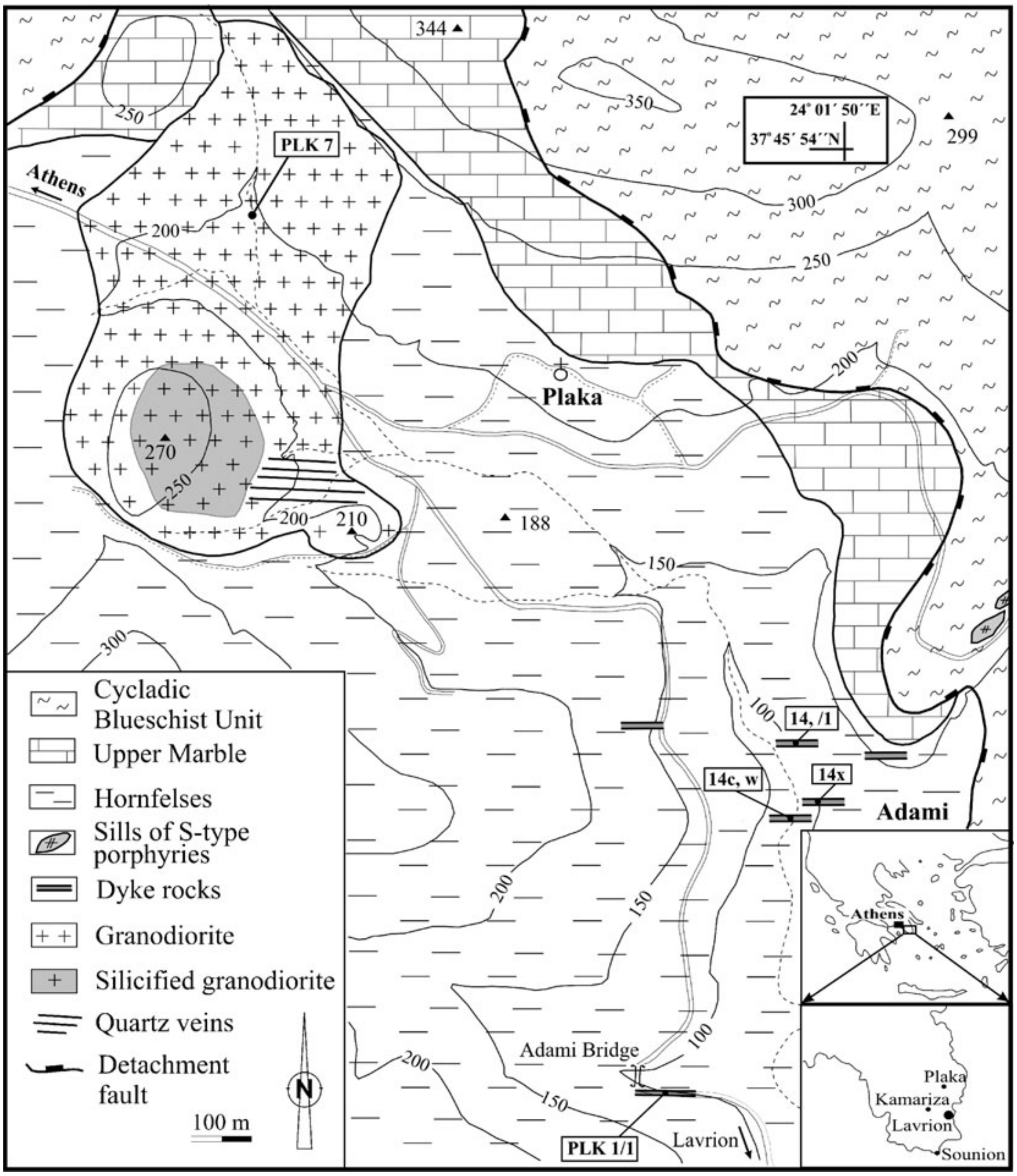

Figure 3. Geological map of Plaka area (thickness and length of dykes not to scale).

4.b. Dykes

Undeformed subvertical dykes of porphyry rocks occur throughout the 'Basal Unit' in the Lavrion area (Fig. 3). They strike WNW–ESE to WSW–ENE and range in composition from quartz-syenite through quartz-monzonite to granodiorite. The width of the known dykes at Plaka and Kamariza varies between 2 and 4 m. Chilled margins are observed in one dyke exposed close to the Adami bridge (Fig. 3). More than five dykes were reported to occur, mainly underground, in the Kamariza area (Campresy, 1889). These dykes range in length from 300 to 900 m. They experienced intense supergene alteration, thus limiting our petrological study to dykes that crop out in the area of Plaka.

5. Petrography

5.a. The granodiorite stock

The fresh granodiorite comprises K-feldspar, plagioclase and biotite. Magnetite, apatite and zircon are accessories. The rock exhibits hydrothermal alteration features along joints fringed by bleached zones containing chlorite, actinolite, epidote and quartz. The major part of the granodiorite stock, including the peripheral portion, is hydrothermally altered. Sericitic alteration and silicification are recognized. The deeper part of the altered portion of the granodiorite stock is cross-cut by a swarm of WNW–ESE-trending quartz veins, whereas the upper part is pervasively silicified.

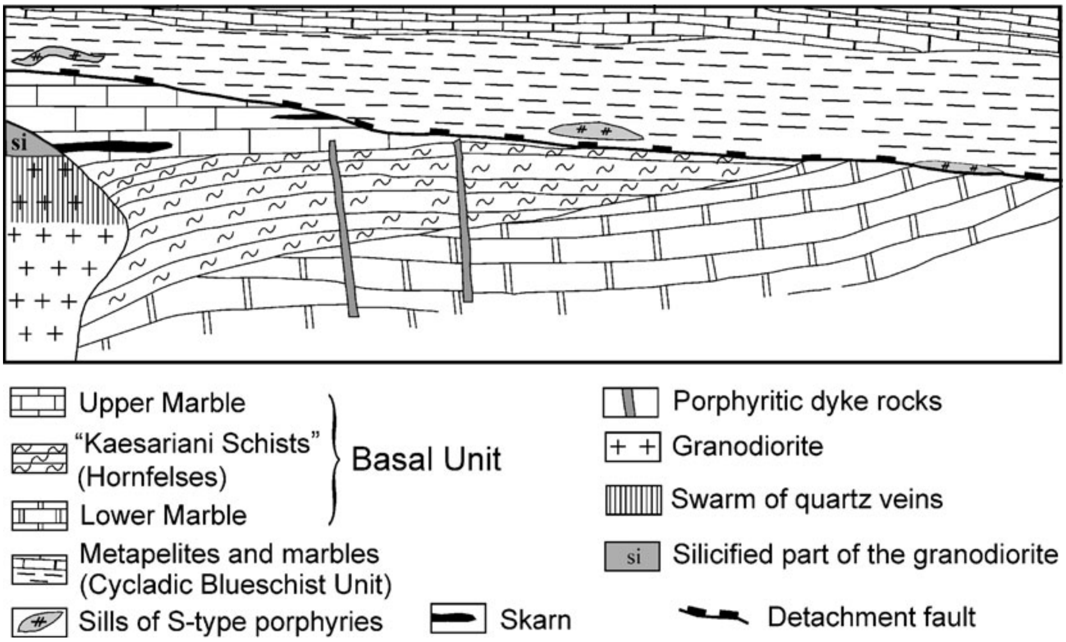

Figure 4. Schematic, roughly NNW–SSE-oriented, tectonostratigraphic section showing the setting of the Miocene intrusive rocks in the Basal Unit and the sills of S-type porphyries (west Plaka area).

Table 1. K–Ar dating on K-feldspar separate

Sample	% K	$^{40}Ar_{rad}$, nl/g	% $^{40}Ar_{air}$	Age (Ma)
GPL 14w	4.96	1.781	16.5	9.4 ± 0.3

5.b. Dykes

Two texturally different types of dyke rocks were observed. The first type (sampled from outcrops along the Adami valley) shows a typical porphyritic texture with phenocrysts of plagioclase, quartz, hornblende and minor ilmenite. The plagioclase is optically zoned. Quartz crystals contain rutile inclusions. Zircon and titanite occur as accessory phases. Primary, green hornblende forms subhedral porphyrocrystals. The groundmass is fine grained and consists of K-feldspar, quartz and plagioclase. Fluidic texture is common. The modal composition of the dykes shows that they range from granodiorite to quartz-monzonite and quartz-syenite. K/Ar dating on a K-feldspar separate yielded an age of 9.4 ± 0.3 Ma (Table 1). Patchy actinolite crystals have formed after primary hornblende. Chlorite, sericite and Fe-oxides are also present.

The second type, cropping out at Adami bridge, displays poikilitic texture. K-feldspar, quartz and poikilitic plagioclase are the main constituents, with ilmenite as the opaque phase. Patchy amphibole crystals (both hornblende and actinolite) are dispersed throughout the groundmass. Accessories are zircon, apatite and titanite. Other secondary phases are chlorite, calcite and minor epidote, occurring either dispersed in the matrix or as thin veinlets. On the basis of modal mineralogy, these samples classify as granites and granodiorites.

6. Mineral chemistry

Representative amphibole and plagioclase analyses are listed in Tables 2 and 3. Analytical methods are described in Appendix 1. Stoichiometric calculations for amphiboles were done on the basis of 23(O) and of 13 cations excluding Ca, Na and K. Igneous amphiboles from the dyke rocks are magnesiohornblendes (nomenclature after Leake *et al.* 1997), whereas their alteration products are mainly actinolites, showing a clear distinction from the primary magnesiohornblendes. The igneous magnesiohornblendes from the dykes differ from the secondary amphiboles in having lower abundances of Si and Ca and higher Ti contents. Primary plagioclases from the dyke rocks are normally zoned, with cores ranging from An_{40} to An_{69} and more sodic rims, ranging from An_{26} to An_{48} (Table 3). Some plagioclase crystals show reverse zoning, with cores ranging from An_{27} to An_{39} and rims whose compositions range from An_{43} to An_{60} (e.g. analyses 9–2c and 9–4r, in Table 3). The orthoclase content is generally low and does not exceed 4.8 wt %. The K-feldspars have orthoclase content from 86.4 to 93.8 wt %.

Pressure estimates for the dyke rocks were made using the Al-in-hornblende geobarometer of Anderson & Smith (1995), but the estimates are imprecise because biotite is absent from the primary assemblage and the analysed plagioclases fall mostly outside the range of $An_{25–35}$ suggested by these authors. Unaltered

https://doi.org/10.1017/S0016756807003949 Published online by Cambridge University Press

Table 2. Representative microprobe analyses of amphiboles of the dyke rocks

Sample	GPL14c	GPL14c	GPL14w	GPL14w	PLK1
Anal. no.	18	20	6	13	18
SiO_2	45.75	47.29	47.04	48.45	51.28
TiO_2	1.41	1.22	1.13	1.07	bdl
Al_2O_3	8.70	7.48	7.88	7.91	3.58
FeO^t	15.60	15.62	13.01	12.93	17.72
MnO	0.71	0.51	0.37	0.35	bdl
MgO	13.15	13.33	14.81	14.76	12.28
CaO	11.40	11.87	11.36	10.85	12.40
Na_2O	1.48	1.11	1.51	1.34	0.53
K_2O	0.69	0.50	0.44	0.39	bdl
Total	98.89	98.93	97.55	98.05	97.79
Structural formulae on the basis of 23 oxygens					
Si	6.585	6.801	6.761	6.869	7.522
Al^{IV}	1.415	1.199	1.239	1.131	0.478
	8.000	*8.000*	*8.000*	*8.000*	*8.000*
Al^{VI}	0.061	0.069	0.096	0.191	0.141
Ti	0.153	0.132	0.122	0.114	–
Fe^{3+}	0.992	0.806	0.899	0.976	0.289
Mg	2.822	2.858	3.173	3.120	2.685
Fe^{2+}	0.886	1.073	0.665	0.557	1.885
Mn	0.087	0.062	0.045	0.042	–
	5.000	*5.000*	*5.000*	*5.000*	*5.000*
Mg	–	–	–	–	–
Fe^{2+}	–	–	–	–	–
Mn	–	–	–	–	–
Ca	1.758	1.829	1.749	1.648	1.949
Na	0.242	0.171	0.251	0.352	0.051
	2.000	*2.000*	*2.000*	*2.000*	*2.000*
Ca	–	–	–	–	–
Na	0.171	0.139	0.170	0.017	0.100
K	0.127	0.092	0.081	0.071	–
	0.298	*0.230*	*0.251*	*0.087*	*0.100*

bdl – below detection limit.

Table 3. Representative microprobe analyses of plagioclases of dyke rocks

Sample	GPL14w	GPL14w	GPL14w	GPL14w	PLK1
Anal. no.	5–2c	5–4r	9–2c	9–4r	3
SiO_2	54.12	58.08	58.05	52.76	54.57
TiO_2	bdl	0.01	bdl	0.03	bdl
Al_2O_3	28.79	25.86	26.06	29.59	27.34
FeO^t	0.19	0.15	0.28	0.35	bdl
MnO	0.04	bdl	0.05	0.05	bdl
MgO	bdl	0.01	bdl	0.03	bdl
CaO	11.45	7.61	7.63	12.55	10.07
Na_2O	4.97	7.02	7.12	4.45	7.65
K_2O	0.15	0.56	0.41	0.23	1.02
Total	99.71	99.31	99.60	100.05	100.65
Structural formulae on the basis of 8 oxygens					
Si	2.452	2.619	2.610	2.394	2.476
Al^{IV}	0.548	0.381	0.390	0.606	0.524
	3.000	*3.000*	*3.000*	*3.000*	*3.000*
Al^{VI}	0.989	0.993	0.991	0.976	0.938
Ti	–	–	–	0.001	–
Fe^t	0.007	0.006	0.010	0.013	–
Mn	0.002	–	0.002	0.002	–
Mg	–	0.001	–	0.002	–
Ca	0.556	0.368	0.368	0.610	0.490
Na	0.436	0.613	0.621	0.392	0.673
K	0.009	0.032	0.024	0.013	0.059
	1.999	*2.013*	*2.016*	*2.009*	*2.160*
Or	0.9	3.2	2.3	1.3	4.8
Ab	43.5	60.5	61.2	38.5	55.1
An	55.6	36.3	36.5	60.3	40.1

bdl – below detection limit; c – core, r – rim.

magnesiohornblende rim compositions from the dyke rocks probably formed at pressures between 3 and 4 kbar.

7. Whole rock chemistry

Chemical analyses of samples from dykes are given in Table 4, along with a single analysis of the Plaka granodiorite stock. We also use the analyses given by Altherr & Siebel (2002) for the same granodiorite stock. Only samples with limited hydrothermal alteration or weathering were analysed. The analysed dyke rocks have experienced weak hydrothermal alteration as evidenced by petrographic observations and the low loss on ignition (LOI) values. The values of the chemical index of alteration, CIA (= molecular $(100^{*}Al_2O_3/(Al_2O_3+CaO^{*}+Na_2O+K_2O))$, where CaO^{*} = molecular $(CaO–3P_2O_5)$), are constant (44.4–52.8; Table 4) and mostly within the range of fresh granites (45–55: Nesbitt & Young, 1982). SiO_2 content ranges between 63.4 and 68.8 % in the dyke rocks and between 66.8 and 70.1 % in the granodiorite stock, while normative corundum lies below 1 % (except sample GPL X with normative corundum = 1.75). The dyke rocks display $K_2O/Na_2O > 1$ (except PLK 1/1 with $K_2O/Na_2O = 0.9$) while the granodiorite stock samples have $K_2O/Na_2O < 1$.

The aluminium saturation index (ASI: molecular $Al_2O_3/(Na_2O+K_2O+CaO)$), remains below 1.1, which is the upper limit for I-type granites and increases with increasing SiO_2 in samples from the dykes and the granodiorite stock (Fig. 5a). The dyke rocks are metaluminous, whereas the Plaka granodiorite stock is metaluminous to slightly peraluminous (Fig. 5b). The peraluminous character shown by the sample GPL X appears to be a consequence of alteration. Figure 6 illustrates selected Harker diagrams for the analysed dyke rocks from Lavrion along with the granodiorite stock on a volatile-free basis. Successive trends are observed from the dykes to the Plaka granodiorite stock. TiO_2, Al_2O_3, MgO and Na_2O show distinctive inflections at around 67 wt % SiO_2. K_2O, Rb, Y and Nb show a continuous decrease with increasing SiO_2, whereas CaO is nearly constant (not shown). Nb and Y contents in the granodiorite stock do not follow the variation defined by the dykes displaying higher values with increasing SiO_2 (Fig. 6).

Spider diagrams of elements normalized to primitive upper mantle (PUM) for the dykes and the granodiorite stock display significant similarities, with marked negative Nb–Ta, P and Ti anomalies while Ba has weak negative anomalies (Fig. 7). The dyke rocks as well as the granodiorite have similar Ocean Ridge Granite (ORG)-normalized patterns, characteristic of volcanic arc granitic rocks (VAG: Pearce, Harris & Tindle, 1984) with low Ta and Nb contents, as well as negative Hf and weak Ba anomalies (not shown).

https://doi.org/10.1017/S0016756807003949 Published online by Cambridge University Press

Table 4. Whole-rock chemical analyses of dyke rocks

	GPL X	GPL 14/1	GPL 14	GPL 14c	GPL 14w	PLK 1/1	PLK 7
Major elements (wt %)							
SiO_2	63.43	64.80	66.12	64.22	64.71	68.80	70.13
TiO_2	0.52	0.60	0.60	0.60	0.59	0.41	0.50
Al_2O_3	15.10	15.50	15.90	15.60	15.40	15.00	15.10
$Fe_2O_3^t$	3.70	3.30	2.10	2.60	3.05	1.60	3.02
MnO	0.24	0.10	0.05	0.06	0.06	0.06	0.05
MgO	1.70	2.20	2.20	2.40	2.20	0.90	0.90
CaO	4.20	3.50	5.20	3.50	4.97	4.37	2.98
Na_2O	1.18	2.18	3.10	1.52	2.80	3.20	3.50
K_2O	3.80	7.50	4.70	9.60	5.44	2.90	3.30
P_2O_5	0.10	0.11	0.12	0.11	0.12	0.11	0.11
LOI	5.60	0.51	0.36	0.25	0.19	2.22	0.52
Total	99.54	100.30	100.43	100.44	99.47	99.57	100.06
CIA	52.81	46.48	45.04	45.04	44.39	48.19	50.98
Trace elements (ppm)							
Cr	31	26	33	24	17	10	10
Rb	152.4	201.2	122.3	247.0	136.4	94.9	99.5
Sr	635.6	340.0	546.7	287.3	529.5	480.2	403.1
Y	21.8	25.4	23.5	24.2	25.3	19.5	24.8
Zr	145.2	173.7	170.9	170.8	180.2	202.6	217.0
Nb	12.6	14.4	13.1	12.9	13.7	12.2	16.3
Cs	8.43	1.09	0.57	1.08	0.65	1.00	1.43
Ba	1072.0	890.1	741.8	1191.0	820.8	660.5	821.2
Hf	3.27	3.84	3.82	3.83	4.05	4.68	2.77
Ta	1.19	1.24	1.22	1.23	1.23	1.13	1.62
Pb	65.2	32.7	27.0	23.9	22.2	13.5	15.8
Th	11.3	13.5	13.2	14.1	13.2	14.3	14.1
U	4.78	5.35	5.48	5.23	5.45	4.40	3.04
REE (ppm)							
La	28.1	23.9	31.0	43.7	33.1	22.3	32.5
Ce	57.6	50.1	60.0	84.7	64.3	44.5	66.1
Pr	6.41	5.75	6.57	9.12	6.95	4.73	7.25
Nd	23.9	22.2	24.2	32.6	26.1	17.1	26.7
Sm	4.60	4.77	4.88	5.71	4.90	3.22	5.27
Eu	0.93	0.79	0.95	0.76	0.95	0.85	1.04
Gd	4.01	4.31	4.31	4.73	4.47	2.90	4.63
Tb	0.60	0.65	0.66	0.66	0.67	0.43	0.70
Dy	3.67	4.00	4.03	4.02	4.04	2.91	4.21
Ho	0.70	0.81	0.77	0.78	0.80	0.61	0.80
Er	2.10	2.35	2.28	2.24	2.29	1.84	2.35
Tm	0.28	0.32	0.32	0.30	0.33	0.28	0.33
Yb	2.02	2.27	2.12	2.09	2.15	1.94	2.09
Lu	0.29	0.34	0.31	0.30	0.33	0.29	0.30

Analysis PLK 7 – sample from the granodiorite stock.

Chondrite normalized rare earth element (REE) patterns for the dyke rocks and the granodiorite stock are illustrated in Figure 8. All the analysed samples are similar with strongly fractionated REE ($(La/Yb)_n = 7.55$–15.00). The LREE are most fractionated, whereas the HREE are essentially flat ($(Tb/Lu)_n = 1.00$–1.58), and all samples show distinct negative Eu anomalies ($Eu/Eu^* = 0.45$–0.67), except one dyke (PLK 1/1) with negligible negative Eu anomaly ($Eu/Eu^* = 0.86$).

8. Sm and Nd isotopes

Sm and Nd isotope determinations were made on two samples of dykes (Table 5). The two ε_{Nd} determinations are identical to within analytical error (−8.6 to −8.7), over a range of SiO_2 contents (on an anhydrous basis) from 65 % to 71 % (Fig. 9). Values of ε_{Nd} are similar to those from plutons in Serifos, Tinos, Mykonos and Ikaria given by Altherr & Siebel (2002). They are slightly more negative than the Western pluton of Naxos, but not as negative as the type II leucogranites of Naxos (Pe-Piper, 2000), suggesting a lesser influence by a crustal component for the Lavrion dykes relative to the leucogranites. The Plaka granodiorite has less strongly negative ε_{Nd} (−7.9 and −7.46) (Juteau, Michard & Albarède, 1986; Altherr & Siebel, 2002) and falls on the same trend of ε_{Nd} v. $^{87}Sr/^{86}Sr$ as the plutonic rocks of Naxos, Mykonos, Tinos and Serifos shown by Pe-Piper (2000) and Altherr & Siebel (2002). The ε_{Nd} of the Plaka granodiorite stock is significantly different from the dyke rocks of Lavrion, however, model ages (based on a depleted mantle model) are identical to within analytical error (1.2 to 1.3 Ga) for all samples, including the Plaka granodiorite.

https://doi.org/10.1017/S0016756807003949 Published online by Cambridge University Press

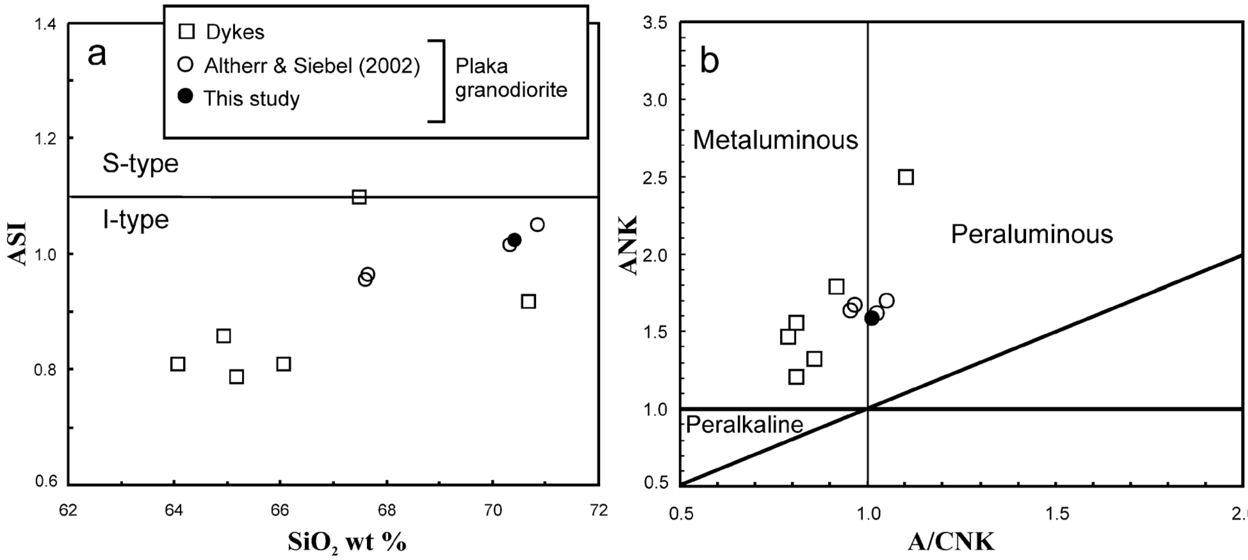

Figure 5. (a) Plot of aluminium saturation index (ASI) ratio v. SiO_2 for the analysed rocks, on a volatile-free basis. (b) Plot of Shand's index (ANK: molar $Al_2O_3/(Na_2O+K_2O)$ v. A/CNK: molar $Al_2O_3/(CaO+Na_2O+K_2O)$) for the analysed dyke rocks and the granodiorite stock (on a volatile-free basis).

9. Discussion

9.a. Petrology, geochemistry

Previous petrological studies have shown that the Cycladic I-type plutons were derived from mixing of two principal sources: a mantle source of mafic and a crustal source of felsic magma. Subsequent evolution of these plutons was dominated by assimilation and fractional crystallization (Altherr *et al.* 1988; Tarney *et al.* 1998; Altherr & Siebel, 2002; Pe-Piper, 2000; Pe-Piper, Piper & Matarangas, 2002).

The dyke rocks and the granodiorite stock from Lavrion show many features of calc-alkaline I-type granitoids: they contain hornblende and titanite, have ASI ≤ 1.1, are generally metaluminous, have normative diopside and low (generally < 1 wt %) normative corundum. In addition, due to their relatively low Nb, Y and Rb contents, on the discrimination diagrams of Pearce, Harris & Tindle (1984) these samples plot in the field of Volcanic Arc Granite (not shown). The negative Ta–Nb anomalies on spider diagrams are typical of I-type granites and of many crustal rocks. Many of these features are characteristic of a subduction-related source, which is also supported by the high-K, calc-alkaline nature of the Lavrion dykes and granodiorite (e.g. Rogers & Hawkesworth, 1989).

The generation of high-K granodioritic to granitic magmas in continental arc settings has been attributed to parent mantle melts that were enriched in subducted-slab-derived fluids and contaminated with crustal material during ascent (e.g. De Paolo, 1981; Hildreth & Moorbath, 1988). Reverse mineral zonation, like that observed in the plagioclases from the dykes, is usually associated with crystal growth in an open system, either a hydrothermal system or a melt after a period of magma mixing or degassing and indicates variations in the conditions local to the crystal (Holten, Jamtveit & Meakin, 2000), compatible with mixing of a mafic and a crustal component during the evolution of the dykes. The small difference in Nd isotopes between the Plaka granodiorite stock and the dykes might be because there was a significant mafic mantle-derived magma component within the stock, whereas the dykes were derived from magma where the contribution of dehydration melting of a crustal component was more important.

The abundance of compatible elements such as Cr in the most mafic dyke rocks is comparable with that of Hercynian paragneisses from Naxos reported by Pe-Piper (2000). These dyke rocks are also clearly enriched in K_2O and Rb, thus indicating that crustal material played an important role in their genesis. Moreover, their REE patterns are remarkably similar to those of the Naxos paragneisses (Fig. 8), suggesting that similar rocks may have been an important source to the magma. Notably, the somewhat peculiar humped pattern among the LREE, which is portrayed by the Naxos paragneisses, appears present in both the dykes and the granodiorite stock.

The investigated rocks show essentially unfractionated HREE patterns, with high $(La/Yb)_n$ and low $(Tb/Yb)_n$ ratios (Fig. 8), as well as high Y and Sr/Y ratios, thus precluding the involvement of substantial amounts of garnet either in the residue during partial melting and final re-equilibration or as part of the fractionating assemblage in the deep crust, consistent with rather low-pressure melting (< 8 kbar). The evolution of the Lavrion dykes and granodiorite into the plagioclase (and K-feldspar) stability field, that is, under crustal conditions, is supported by the negative

https://doi.org/10.1017/S0016756807003949 Published online by Cambridge University Press

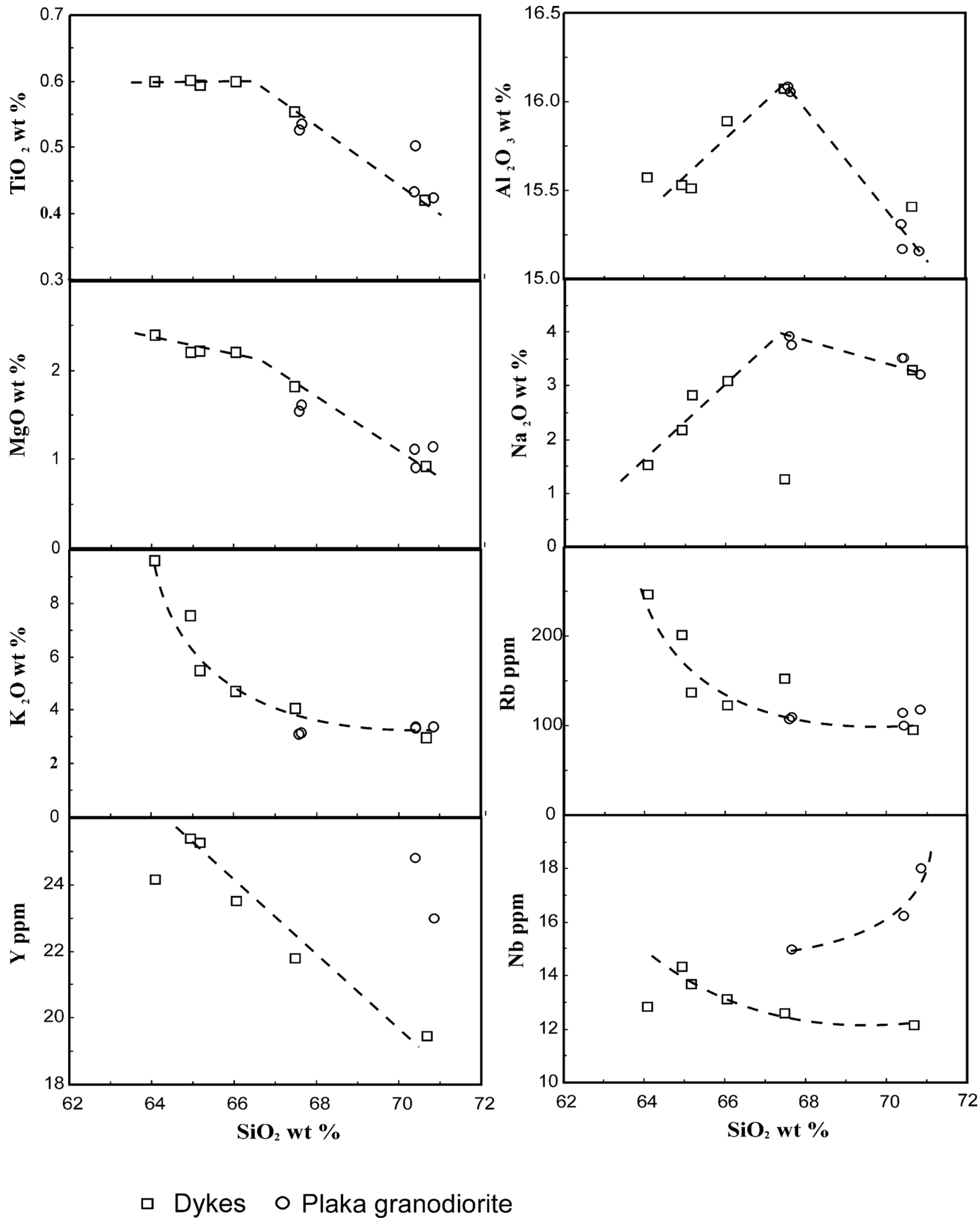

Figure 6. Selected Harker variation diagrams of elements v. SiO_2 for the analysed rocks (on a volatile-free basis).

Ba, Eu and P anomalies on primitive upper mantle-normalized plots (Fig. 7).

The systematic variation on the Harker diagrams for the dykes and the granodiorite stock may be the result of mixing, as discussed above, and of fractional crystallization. The Na_2O and Al_2O_3 distributions (Fig. 6), as well as the negative Eu anomalies (Fig. 8), suggest that sodic plagioclase fractionation became important during the late stages of evolution of the dykes and the formation of the granodiorite. The small Eu anomaly in sample PLK 1/1 is interpreted to be due to the strong contribution of hornblende fractionation that minimizes the Eu anomaly (Henderson, 1984). The continuous decreases of MgO, Y and Nb are compatible with hornblende separation during the evolution of the dyke rocks. The TiO_2 inflection at around 67 wt % silica is likely to indicate the onset of fractionation of titanite. The influence of hornblende and titanite fractionation is moreover indicated by the negative anomalies in Nb and Ti, respectively, on spider diagrams, whereas the P negative anomaly should result from apatite (and possibly hornblende) separation. K_2O and Rb show a continuous decrease, indicating that possibly K-feldspar and biotite were significant crystallizing phases in these rocks; the observed negative Ba anomalies on the spider diagrams

https://doi.org/10.1017/S0016756807003949 Published online by Cambridge University Press

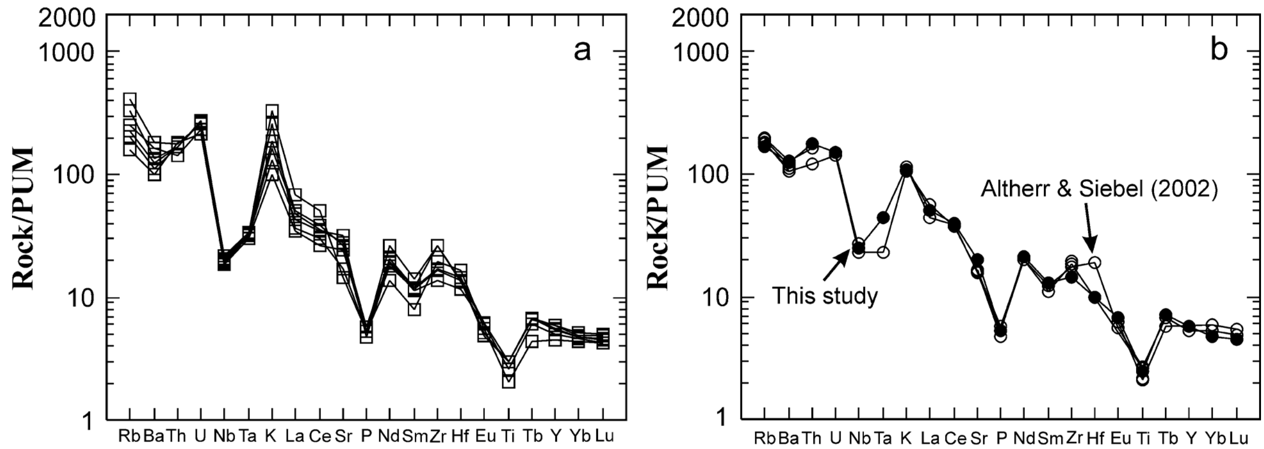

Figure 7. Primitive Upper Mantle-normalized spider diagrams for: (a) the dyke rocks (this study) and (b) the granodiorite stock (data from Altherr & Siebel, 2002 and this study). Normalizing values after Sun & McDonough (1989).

are consistent with this interpretation. The higher Nb and Y values in the granodiorite stock relative to that expected from the trend defined by the dykes may be a consequence of mixing with a mantle derived magma, discussed earlier.

9.b. Geodynamic implications

The igneous rocks of the Lavrion area represent the northwesternmost outcrop of Miocene intrusions in the Attic–Cycladic belt. Previous authors have regarded the Late Miocene motion on the old thrust fault separating the Blueschist and Basal units as compressive (renewed thrusting). However, regionally, extensional (detachment) faulting predominated at this time. The metamorphic grade in the Basal Unit, where there is a widespread thermal aureole produced by a rather small intrusion, appears to be substantially higher than in the Blueschist Unit, which escaped contact metamorphism. Final emplacement of the Blueschist over the Basal unit took place at rather shallow depths, post-dating contact metamorphism of the rocks of the Basal Unit, and this abrupt decrease in metamorphic grade is consistent with the regional presence of extensional detachment faulting.

The general E–W orientation of the dykes (WNW–ESE to WSW–ENE) indicates a regional extensional stress field with a roughly N–S direction. The exact mode of occurrence of the granodioritic body at depth is unknown, while the poor exposure of intrusive contacts renders the study of the mode of emplacement difficult. Based on measurement of orientation of the long axis of plagioclase crystals, a N–S direction of magma flow was concluded by Theodoropoulos & Fytrolakis (1974), implying some form of structural control on the intrusion. By analogy with observations in Delos (Pe-Piper, Piper & Matarangas, 2002) and Naxos (Koukouvelas & Kokkalas, 2003), where early stages of pluton emplacement took place along wrench faults parallel to the extension direction of a major mid-crustal detachment fault, the Plaka stock may have been emplaced along a wrench fault within a regional N–S extensional setting. The numerous wide WNW–ESE-oriented quartz veins (tension gashes) cutting the hydrothermally altered granodiorite further indicate substantial extension in the footwall after granodiorite emplacement. The lack of dykes in the granodiorite suggests that they are older that the granodiorite. It seems that extension and the exhumation of the metamorphic units was accompanied at a late stage by the intrusion first of the dykes, following WNW–SSE-trending high-angle normal faults, and then the granodiorite.

The 9.4 ± 0.3 Ma K–Ar age on feldspar for the dyke rock in the footwall is probably the isotopic age determination closest to the emplacement age and provides a minimum age for igneous activity, whereas the progressively younger ages of 8.27 ± 0.11 Ma obtained from biotite and of 7.3 Ma on apatite by fission track (Altherr *et al.* 1982) are cooling ages. This progressive cooling points to unroofing that is most easily achieved by extensional detachment faulting. In this case there was the same extension direction before granodiorite emplacement (to produce the dykes) and after granodiorite emplacement (to produce the widespread quartz veins).

The NNE–SSW orientation of the Late Miocene extensional stress field is further confirmed by the orientation of WNW–ESE-trending mineralized tension gashes, explored underground at Plaka. These are filled with banded hydrothermal Pb–Ag–Zn sulphide mineralization steeply SSW dipping, cutting hornfelses that were pervasively hydrothermally altered (Skarpelis, 2002). They form a set of fractures probably associated with continued extension, cooling of the granodiorite and generation of hydrothermal fluids post-dating skarn formation.

Regional considerations suggest that this extension was regional rather than being local or related to the structural evolution of the Basal Unit in the Lavrion

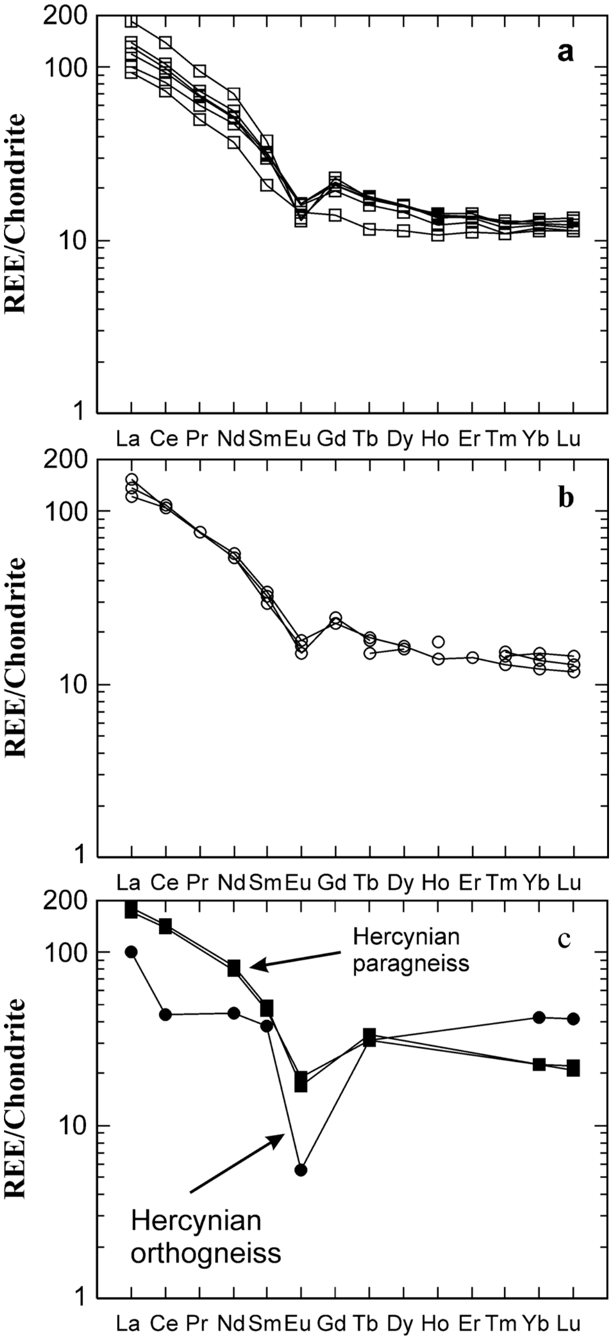

Figure 8. Chondrite-normalized REE patterns for: (a) the dyke rocks (this study), (b) the granodiorite stock (data from Altherr & Siebel, 2002 and this study) and (c) the Hercynian, Naxos paragneiss and orthogneiss for comparison (after Pe-Piper, 2000).

area. Structural analysis of Miocene to Pliocene sedimentary sequences in Attica and Beotia suggests they were deposited in basins bounded mainly by E–W-trending faults (A. Mettos, unpub. Ph.D. thesis, Univ. Athens, 1992) formed as a result of N–S extension.

The geodynamic evolution of the Lavrion area has many features in common with that of NE Attica, the central Aegean islands and southern Evia. An extension direction of NNE inferred from dyke orientations and the fold axes of Blueschist Unit rocks in Lavrion is parallel to the regional ductile shear directions from NE Attica, southern Evia, Andros and Kea in greenschist facies (St. Lozios, unpub. Ph.D. thesis, Univ. Athens, 1993; P. Gautier, unpub. Ph.D. thesis, Univ. Rennes I, 1995; Walcott, 1998). This observation does not demonstrate extension rather than thrusting, but does place Lavrion within a regional context.

Late granitic to dioritic dykes trending roughly E–W cut through the granodiorite and country rocks in Serifos island, where earlier ductile structures trend NE–SW (Salemink, 1985; Petrakakis *et al.* 2004). A zircon fission track age of 8.6 ± 1.6 Ma, obtained on a sample of a dyke within the metamorphic aureole, was interpreted as cooling age (St. Brichau, unpub. Ph.D. thesis, Univ. Mainz & Univ. Montpellier II, 2004). Based on age and style of emplacement, these dykes seem to correlate with the dyke rocks of the Lavrion area.

Emplacement of the Blueschist Unit over the Basal Unit at Lavrion by extensional detachment likely took place in Late Miocene times, on the basis of the cooling ages for the igneous rocks (8.3 Ma on biotite, 7.3 Ma on apatite: Altherr *et al.* 1982). By comparison, in Naxos, unroofing of the footwall is dated at 8.2 Ma on apatite (e.g. Altherr *et al.* 1982), and in Paros, Ikaria, Mykonos and Serifos the detachment faults started to operate at *c.* 13 Ma (e.g. Kumerics *et al.* 2005, Brichau *et al.* 2006), suggesting that the timing of the extensional fault system of Lavrion was similar to that in the central Cyclades and therefore evolved before, during and after the intrusion of the dykes and the granodiorite stock.

10. Conclusions

The igneous rocks of the Lavrion area represent the northwesternmost outcrop of Miocene intrusions in the Attic–Cycladic belt. The 9.4 ± 0.3 Ma age on feldspar for the dyke rock provides a minimum age for the igneous activity in the Lavrion area. The orientation, both of the dykes of porphyry rocks and the quartz veins (tension gashes) cutting the hydrothermally altered granodiorite stock, indicates a regional extensional stress field with roughly N–S direction. Extension, emplacement of the granitoid rocks, and the exhumation of the metamorphic units were the result of regional extension and detachment faulting continuous with the well-known extension of the Cyclades. Final emplacement of the Blueschist Unit over the Basal Unit took place at rather shallow depths, post-dating contact metamorphism of the rocks of the Basal Unit.

Various geochemical and mineralogical criteria indicate that the main geochemical features of the granitoid rocks evolved under crustal pressure conditions. Small differences in Sm–Nd isotope systematics suggest that the granodiorite stock may have a greater component of mantle source material than the dykes,

https://doi.org/10.1017/S0016756807003949 Published online by Cambridge University Press

Table 5. Sm and Nd isotope data for the igneous rocks

Sample	Sm (ppm)	Nd (ppm)	$^{147}Sm/^{144}Nd$	$^{143}Nd/^{144}Nd$	ε_{Nd} (I)$^{+}$	T_{DM}(Ga)
GPL 14W	5.53	29.26	0.1143	0.512186 ± 06	−8.71	1.31
PLK 1/1	3.26	18.82	0.1047	0.512192 ± 05	−8.58	1.20
Lau 3*	4.98	25.00	0.1229	0.512251 ± 01	−7.46	1.33

For T_{DM} ages determinations the equation used is that of Faure (1986). For ε_{Nd} determinations we used the constants: $^{143}Nd/^{144}Nd = 0.512638$ and $^{147}Sm/^{144}Nd = 0.1967$. Errors for Nd isotopic compositions represent 2 sigma of the mean based on in-run statistics.
*Data from Altherr & Siebel (2002).
$^{+}$The ages (Ma) used for ε_{Nd} (I) calculations are as those in Altherr & Siebel (2002): 9 Ma for Serifos, 10 Ma for Lavrion and Kos, 11 Ma for Mykonos and Delos, 12 Ma for Naxos, Ikaria and Samos and 15 Ma for Tinos.

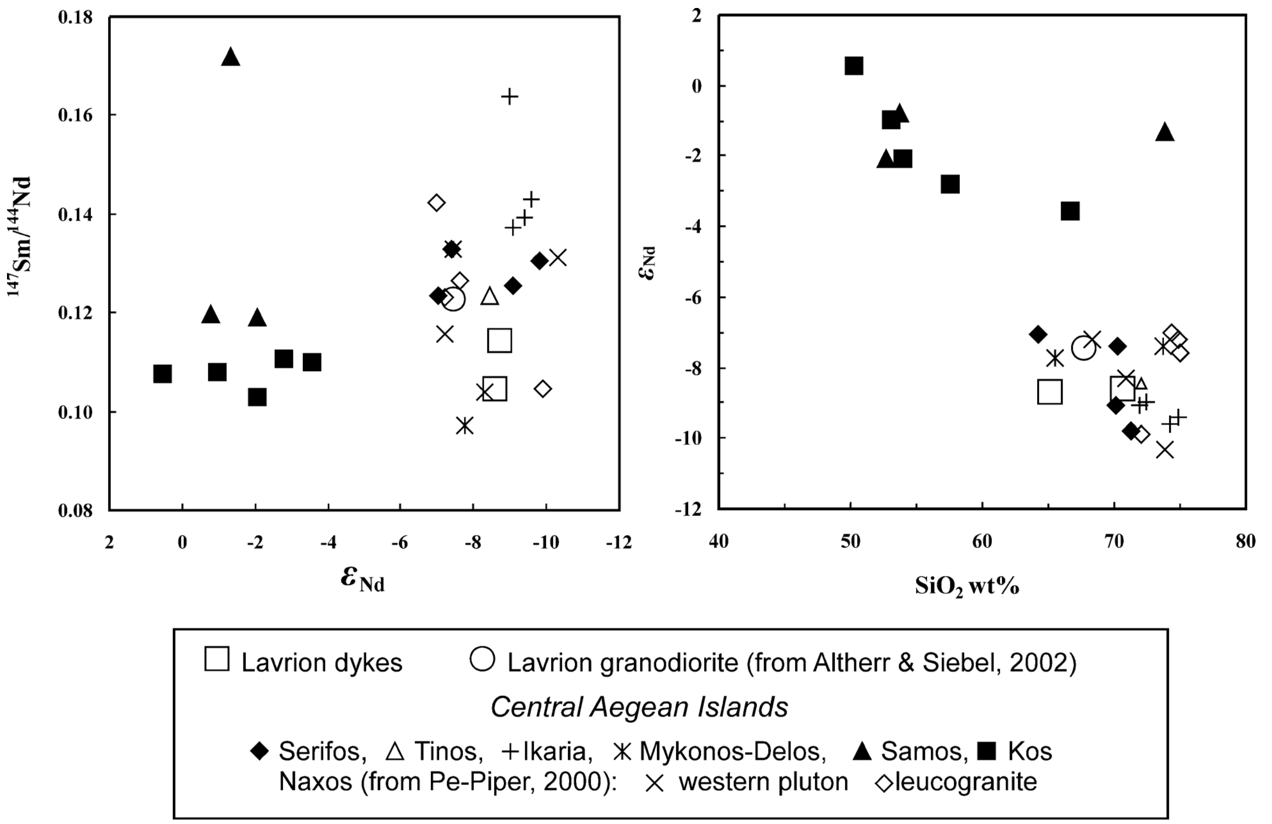

Figure 9. Plots of $^{147}Sm/^{144}Nd$ v. ε_{Nd} and ε_{Nd} v. SiO_2 for the Lavrion igneous rocks, the Central Aegean plutons (after Altherr & Siebel, 2002), and the western pluton and the leucogranite of Naxos (after Pe-Piper, 2000).

but that both had an important felsic component of crustal origin. In detail, the LILE in the dykes resemble those of Hercynian paragneisses which have been interpreted as an important component of granitoid dykes on Naxos. Continuous geochemical trends from the dykes to the Plaka granodiorite stock are interpreted principally in terms of fractional crystallization of sodic plagioclase, hornblende, titanite and possibly K-feldspar and biotite.

Acknowledgements. This work was supported in part by the 'Special Account for Research Grants, National and Kapodistrian University of Athens' (grant 4/6424 to N.S.). The work on mineral chemistry was carried out during a stay by N.S. with the Department of Earth and Environmental Sciences, Ludwig Maximilians University of Munich. Professor Rudolf Höll is thanked for helpful discussions and hospitality when in Munich. Thanks are due to Professors Robert Marschik and Thomas Fehr for making available laboratory facilities. We also thank Dr D. J. W. Piper for his valuable comments on the paper. Reviews by Professor R. Altherr and an anonymous referee resulted in substantial improvements to this manuscript and are greatly appreciated. Thanks are due to Dr Sofia Karipi for help with drawing Figures 1 through 4.

References

Altherr, R., Henjes-Kunst, F., Matthews, A., Friedrichsen, H. & Hansen, B. T. 1988. O–Sr isotopic variations in Miocene granitoids from the Aegean: Evidence for an origin by combined assimilation and fractional crystallization. *Contributions to Mineralogy and Petrology* **100**, 528–41.
Altherr, R., Kreuzer, H., Lenz, H., Wendt, I., Harre, W. & Dürr, S. 1994. Further evidence for a Late Cretaceous

low pressure high temperature terrane in the Cyclades, Greece. *Chemie der Erde* **54**, 319–28.

ALTHERR, R., KREUZER, H., WENDT, I., LENZ, H., WAGNER, G. A., KELLER, J., HARRE, W. & HOHNDORF, A. 1982. A Late Oligocene/Early Miocene high temperature belt in the Attic–Cycladic crystalline complex (SE Pelagonian, Greece). *Geologisches Jahrbuch* **E23**, 97–164.

ALTHERR, R., SCHLIESTEDT, M., OKRUSCH, M., SEIDEL, E., KREUZER, H., HARRE, W., LENZ, H., WENDT, I. & WAGNER, G. A. 1979. Geochronology of high-pressure rocks on Sifnos (Cyclades, Greece). *Contributions to Mineralogy and Petrology* **70**, 245–55.

ALTHERR, R. & SIEBEL, W. 2002. I-type plutonism in a continental back-arc setting: Miocene granitoids and monzonites from the central Aegean Sea, Greece. *Contributions to Mineralogy and Petrology* **143**, 397–415.

ANDERSON, J. L. & SMITH, D. R. 1995. The effects of temperature and fO_2 on the Al-in-hornblende barometer. *American Mineralogist* **80**, 549–59.

AVIGAD, D. & GARFUNKEL, Z. 1989. Low angle faults above and below a blueschist belt, Tinos island, Cyclades, Greece. *Terra Nova* **1**, 182–7.

AVIGAD, D., GARFUNKEL, Z., JOLIVET, L. & AZANON, J. M. 1997. Back arc extension and denudation of Mediterranean eclogites. *Tectonics* **16**, 924–41.

BALTATZIS, E. 1981. Contact metamorphism of a calc-silicate hornfels from Plaka area, Laurium, Greece. *Neues Jahrbuch für Mineralogie Monatshefte* **11**, 481–8.

BALTATZIS, E. 1996. Blueschist-to-greenschist transition and the P–T path of prasinites from the Lavrion area, Greece. *Mineralogical Magazine* **60**, 551–61.

BAZIOTIS, I., MPOSKOS, E. & PERDIKATSIS, V. 2006. Reconstruction and correlation of the exhumation history of high-pressure/low-temperature metamorphic rocks from Attica. *NECAM 2006 – International Conference on Neogene Magmatism of the Central Aegean and Adjacent Areas, Book of Abstracts*, p. 28.

BÖGER, H. 1983. Stratigraphische und tectonische Verknuepfungen kontinentaler Sedimente des Neogens im Aegais-Raum. *Geologische Rundschau* **72**, 771–813.

BRICHAU, S., RING, U., KETCHAM, R. A., CARTER, A., STOCKLI, D. & BRUNEL, M. 2006. Constraining the long-term evolution of the slip rate for a major extensional fault system in the central Aegean, Greece, using thermochronology. *Earth and Planetary Science Letters* **24**, 293–306.

BRÖCKER, M., BIELING, D., HACKER, B. & GANS, P. 2004. High-Si phengites record the time of greenschist-facies overprinting: implications for models suggesting mega-detachments in the Aegean Sea. *Journal of Metamorphic Geology* **22**, 427–42.

BRÖCKER, M. & ENDERS, M. 1999. U–Pb zircon geochronology of unusual eclogite facies rocks from Syros and Tinos (Cyclades, Greece). *Geological Magazine* **136**, 111–18.

BRÖCKER, M. & FRANZ, L. 1994. The Contact Aureole on Tinos (Cyclades, Greece). Part I: Field Relationships, Petrography and P–T Conditions. *Chemie der Erde* **54**, 262–80.

BRÖCKER, M. & FRANZ, L. 1998. Rb–Sr isotope studies on Tinos Island (Cyclades, Greece): Additional time constraints for metamorphism, extent of infiltration-controlled overprinting and deformational activity. *Geological Magazine* **135**, 369–82.

BRÖCKER, M. & KEASLING, A. 2006. Ionprobe U–Pb zircon ages from the high-pressure/low-temperature mélange of Syros, Greece: age diversity and the importance of pre-Eocene subduction. *Journal of Metamorphic Geology* **24**, 615–31.

BRÖCKER, M., KREUZER, H., MATTHEWS, A. & OKRUSCH, M. 1993. $^{39}Ar/^{40}Ar$ and oxygen isotope studies of polymetamorphism from Tinos island, Cycladic blueschist belt, Greece. *Journal of Metamorphic Geology* **11**, 223–40.

BUICK, I. S. 1991. The late Alpine evolution of an extensional shear zone, Naxos, Greece. *Journal of the Geological Society, London* **148**, 93–103.

CAMPRESY, A. 1889. Le Laurium. *Revue Univ. des Mines* **6**, Liége, Paris.

DE PAOLO, D. J. 1981. Trace element and isotopic effects of combined wall rock assimilation and fractional crystallization. *Earth and Planetary Science Letters* **53**, 189–202.

DERMITZAKIS, M. & PAPANIKOLAOU, D. 1980. The molasse of Paros island, Aegean Sea. *Annalen des Naturhistorischen Museums in Wien* **83**, 59–71.

DUBOIS, R. & BIGNOT, G. 1979. Presence d'un "hard-ground" nummulitique au sommet de la serie cretacée d'Almyropotamos (Eubée méridionale, Grèce). Conséquences. *Comptes Rendu de l'Academie des Sciences de Paris* **289** D, 993–5.

DÜRR, S. & ALTHERR, R. 1979. Existence de klippes d'une nappe composite néogéne dans l'île de Mykonos/Cyclades (Grèce). *Rapports de la Commission Internationale de la Mer Méditerranée*, **25/62**, 33–4.

DÜRR, S., ALTHERR, R., KELLER, J., OKRUSCH, M. & SEIDEL, E. 1978. The median Aegean crystalline belt: stratigraphy, structure, metamorphism, magmatism. In *Alps, Apennines, Hellenides* (eds H. Cloos, D. Roeder & K. Schmidt), pp. 455–76. Stuttgart: Schweizerbart.

FAURE, G. 1986. *Principles of isotope geology*, 2nd ed. New York: John Wiley, 589 pp.

FAURE, M., BONNEAU, M. & PONS, J. 1991. Ductile deformation and syntectonic granite emplacement during the late Miocene extension of the Aegean (Greece). *Bulletin Société Géologique de France* **162**, 3–11.

GAUTIER, P. & BRUN, J. P. 1994. Crustal-scale geometry and kinematics of late orogenic extension in the central Aegean (Cyclades and Evia island). *Tectonophysics* **238**, 399–424.

HENDERSON, P. 1984. *Rare Earth Element geochemistry*. Amsterdam: Elsevier, 510 pp.

HILDRETH, W. & MOORBATH, S. 1988. Crustal contributions to arc magmatism in the Andes of Central Chile. *Contributions to Mineralogy and Petrology* **98**, 455–89.

HOLTEN, T., JAMTVEIT, B. & MEAKIN, P. 2000. Noise and oscillatory zoning of minerals. *Geochimica et Cosmochimica Acta* **64**, 1893–1904.

JOLIVET, L., FACCENNA, C., GOFFÉ, B., BUROV, E. & ACARD, F. 2003. Subduction tectonics and exhumation of high-pressure metamorphic rocks in the Mediterranean orogens. *American Journal of Science* **303**, 353–409.

JUTEAU, M., MICHARD, A. & ALBARÈDE, F. 1986. The Pb–Sr–Nd isotope geochemistry of some recent circum Mediterranean granites. *Contributions to Mineralogy and Petrology* **92**, 331–40.

KATSIKATSOS, G. 1977. La structure tectonique d'Attique et de l'île d'Eubée. In *Proceedings of the VI Colloquium on the Geology of the Aegean Region* (ed. G. Kallergis), pp. 211–28. I.G.M.R., Athens, 1.

KATSIKATSOS, G., MIGIROS, G., TRIANTAFYLLIS, M. & METTOS, A. 1986. *Geological structure of Internal Hellenides (E. Thessaly–SW Macedonia, Euboea–Attica–Northern Cyclades Islands and Lesbos)*. Geological and Geophysical Research, Special Issue, I.G.M.E., Athens.

KATZIR, Y., MATTHEWS, A., GARFUNKEL, Z., SCHLIESTEDT, M. & AVIGAD, D. 1996. The tectono-metamorphic evolution of a dismembered ophiolite (Tinos, Cyclades, Greece). *Geological Magazine* **133**, 237–54.

KESSEL, G. 1990. Untersuchungen zur Deformation und Metamorphose in Attischen Krystallin, Griechenland. *Berliner Geowissenschaftlicher Abhandlungen* **A126**, 1–150.

KOUKOUVELAS, I. K. & KOKKALAS, S. 2003. Emplacement of the Miocene west Naxos pluton (Aegean Sea, Greece): a structural study. *Geological Magazine* **140**, 45–61.

KUMERICS, C., RING, U., BRICHAU, ST., GLODNY, J. & MONIE, P. 2005. The extensional Messaria shear zone and associated brittle detachment faults, Aegean Sea, Greece. *Journal of the Geological Society, London* **162**, 701–21.

LEAKE, B. E., WOOLEY, A. R., ARPS, C. E. S., BIRCH, W. D., GILBERT, M. C., GRICE, J. D., HAWTHORNE, F. C., KATO, A., KISCH, H. J., KRIVOVICHEV, V. G., LINTHOUT, K., LAIRD, J., MANDARINO, J., MARESCH, W. V., NICKEL, E. H., ROCK, N. M. S., SCHUMACHER, J. C., SMITH, D. C., STEPHENSON, N. C. N., UNGARETTI, L., WHITTAKER, E. J. W. & YOUZHI, G. 1997. Nomenclature of amphiboles; report of the Subcommittee on amphiboles of the International Mineralogical Association Commission on New Minerals and Mineral Names. *European Journal of Mineralogy* **9**, 623–51.

LEE, J. & LISTER, G. S. 1992. Late Miocene ductile extension and detachment faulting, Mykonos, Greece. *Geology* **20**, 121–4.

LELEU, M. & NEUMANN, M. 1969. L'âge des formations d'Attique: du paleozoique au mesozoique. *Comptes Rendu de l'Academie des Sciences de Paris* **268**, 1361–3.

LISTER, G. S., BANGA, G. & FEENSTRA, A. 1984. Metamorphic core complexes of the Cordilleran type in the Cyclades, Aegean Sea, Greece. *Geology* **12**, 221–5.

MARINOS, G. P. 1971. On the radiodating of Greek rocks (in Greek, English summary). *Annales Géologiques des Pays Hélleniques* **23**, 175–82.

MARINOS, G. P. & MAKRIS, J. 1975. Geological and geophysical considerations of new mining possibilities in Laurium, Greece. *Annales Géologiques des Pays Hélleniques* **27**, 1–10.

MARINOS, G. P. & PETRASCHECK, W. E. 1956. *Laurium*. Geological & Geophysical Research 4/1, Institute for Geology and Subsurface Research, 1–247.

MEZGER, K., ALTHERR, R., OKRUSCH, M., HENJES-KUNST, F. & KREUZER, H. 1985. Genesis of acid/basic rock associations: a case study. The Kallithea intrusive complex, Samos, Greece. *Contributions to Mineralogy and Petrology* **90**, 353–66.

MINOUX, L., BONNEAU, M. & KIENAST, J. R. 1980. L'île d'Amorgos une fenêtre des zones externes, au coeur de l'Egée (Gréce), métamorphisée dans le faciés schistes bleus. *Comptes Rendu de l'Academie des Sciences de Paris* **291** D, 745–8.

NESBITT, H. W. & YOUNG, G. M. 1982. Early Proterozoic climates and plate motions inferred from major element chemistry of lutites. *Nature* **299**, 715–17.

OKRUSCH, M. & BRÖCKER, M. 1990. Eclogite facies rocks in the Cycladic blueschist belt, Greece: A review. *European Journal of Mineralogy* **2**, 451–78.

PAPANIKOLAOU, D. 1987. Tectonic evolution of the Cycladic blueschist belt (Aegean sea, Greece). In *Chemical Transport in Metasomatic Processes* (ed. H. C. Helgeson), pp. 429–50. Dordrecht: Reidel Publishing Company.

PAPANIKOLAOU, D. & SYSKAKIS, D. 1991. Geometry of acid intrusives in Plaka, Laurium and relation between magmatism and deformation. *Bulletin of the Geological Society of Greece* **25**(1), 355–68.

PARRA, T., VIDAL, O. & JOLIVET, L. 2002. Relation between the intensity of deformation and retrogression in blueschist metapelites of Tinos Island (Greece) evidenced by chlorite-mica local equilibria. *Lithos* **63**, 41–66.

PEARCE, J. A., HARRIS, N. B. W. & TINDLE, A. G. 1984. Trace element discrimination diagrams for the tectonic interpretation of granitic rocks. *Journal of Petrology* **25**, 956–83.

PE-PIPER, G. 2000. Origin of S-type granites coeval with I-type granites in the Hellenic subduction system, Miocene of Naxos, Greece. *European Journal of Mineralogy* **12**, 859–75.

PE-PIPER, G. & PIPER, D. J. W. 2004. Miocene igneous rocks of Samos: magma evolution during continental back-arc extension. *Proceedings 5th International Symposium on Eastern Mediterranean Geology, Thessaloniki, April 2004*, 1212–15.

PE-PIPER, G., PIPER, D. J. W. & MATARANGAS, D. 2002. Regional implications of geochemistry and style of emplacement of Miocene I-type diorite and granite, Delos, Cyclades, Greece. *Lithos* **60**, 47–66.

PETRAKAKIS, K., GRASEMANN, B., IGLSEDER, C., RAMBOUSEK, C. & ZAMOLYI, A. 2004. Deformation and magmatism on the island of Serifos, western Cyclades. *Proceedings 5th International Symposium on Eastern Mediterranean Geology, Thessaloniki, April 2004*, 1228–31.

REINECKE, T., ALTHERR, R., HARTUNG, B., HATZIPANAGIOTOU, K., KREUZER, H., HARRE, W., KLEIN, H., KELLER, J., GEENEN, E. & BÖGER, H. 1982. Remnants of a Late Cretaceous high temperature belt on the island of Anafi (Cyclades, Greece). *Neues Jarhbuch für Mineralogie Abhandlungen* **145**, 157–82.

RING, U. & LAYER, P. W. 2003. High-pressure metamorphism in the Aegean, eastern Mediterranean: Underplating and exhumation from the Late Cretaceous until the Miocene to Recent above the retreating Hellenic subduction zone. *Tectonics* **22**(3), doi:10.1029/2001TC001350, 23 pp.

RING, U., LAYER, P. W. & REISCHMANN, T. 2001. Miocene high-pressure metamorphism in the Cyclades and Crete, Aegean Sea, Greece: Evidence for large-scale magnitude displacement on the Cretan detachment. *Geology* **29**, 395–8.

RING, U. & REISCHMANN, T. 2002. The weak and superfast Cretan detachment, Greece: exhumation at subduction rates in extruding wedges. *Journal of the Geological Society, London* **159**, 225–8.

ROGERS, G. & HAWKESWORTH, C. J. 1989. A geochemical traverse across the North Chilean Andes: evidence for crust generation from the mantle wedge. *Earth and Planetary Science Letters* **91**, 271–85.

SALEMINK, J. 1985. Skarn and ore formation at Seriphos, Greece. *Geologica Ultraiectina* **40**, 1–231.

https://doi.org/10.1017/S0016756807003949 Published online by Cambridge University Press

SÁNCHEZ-GÓMEZ, M., AVIGAD, D. & HEIMANN, A. 2002. Geochronology of clasts in allochthonous Miocene sedimentary sequences on Mykonos and Paros Islands: implications for back-arc extension in the Aegean Sea. *Journal of the Geological Society, London* **159**, 45–60.
SHAKED, Y., AVIGAD, D. & GARFUNKEL, Z. 2000. Alpine high-pressure metamorphism at the Almyropotamos window (southern Evia, Greece). *Geological Magazine* **137**, 367–80.
SKARPELIS, N. 2002. Geodynamics and evolution of the Miocene mineralization in the Cycladic–Pelagonian belt, Hellenides. *Bulletin of the Geological Society of Greece* **34**(6), 2191–206.
SKARPELIS, N., KYRIAKOPOULOS, K. & VILLA, I. 1992. Occurrence and $^{40}Ar/^{39}Ar$ dating of a granite in Thera (Santorini, Greece). *Geologische Rundschau* **81**, 729–35.
SKARPELIS, N. & LIATI, A. 1990. The prevolcanic basement of Thera at Athinios: Metamorphism, Plutonism and Mineralisation. In *Thera and the Aegean World III*, 2 (ed. D. A. Hardy), pp. 172–82. London: The Thera Foundation.
SUN, S. S. & MCDONOUGH, W. F. 1989. Chemical and isotopic systematics of oceanic basalts: implications for mantle composition and processes. In *Magmatism in the Oceanic Basins* (eds A. D. Saunders & M. J. Norry), pp. 313–45. Geological Society of London, Special Publication no. 42.
TARNEY, J., BARR, S. R., MITROPOULOS, P., SIDERIS, K., KATERINOPOULOS, A. & STOURAITI, C. 1998. Santorini: Geochemical constraints on magma sources and eruption mechanisms. In *Proceedings 2nd Workshop: "The European Laboratory Volcanoes"* (eds R. Casale, M. Fytikas, G. Sigvaldasson & G. Vougioukalakis), pp. 89–111. Brussels: European Commission, Directorate-General Science.
THEODOROPOULOS, D. & FYTROLAKIS, N. 1974. Beitrag zur Kenntnis der Jungtectonik des Gebietes von Plaka bei Lavrion. *Mining Metallurgical Annales* **18**, 29–34.
TOMASCHEK, F., KENNEDY, A. K., VILLA, I. M., LAGOS, M. & BALLHAUS, C. 2003. Zircons from Syros, Cyclades, Greece – Recrystallization and mobilization of zircon during high-pressure metamorphism. *Journal of Petrology* **44**, 1977–2002.
TROTET, F., VIDAL, O. & JOLIVET, L. 2001. Exhumation of Syros and Sifnos metamorphic rocks (Cyclades, Greece). New constraints on the *P–T* paths. *European Journal of Mineralogy* **13**, 901–20.
WALCOTT, C. R. 1998. The Alpine evolution of Thessaly (NW Greece) and late Tertiary Aegean kinematics. *Geologica Ultraiectina* **162**, 1–176.
WASSERBURG, G. J., JACOBSEN, S. B., DE PAOLO, D. J., MCCULLOCH, M. T. & WEN, T. 1981. Precise determination of Sm/Nd ratio, Sm, Nd isotopic abundances in standard solutions. *Geochimica et Cosmochimica Acta* **45**, 2311–23.
WIJBRANS, J. R. & MCDOUGALL, I. 1988. Metamorphic evolution of the Attic–Cycladic Metamorphic Belt on Naxos (Cyclades, Greece) utilizing $^{40}Ar/^{39}Ar$ age spectrum measurements. *Journal of Metamorphic Geology* **6**, 571–94.

Appendix 1. Analytical methods

The principal outcrops of granitoid rocks were studied in the field and representative samples were collected. Microprobe analyses of minerals were performed on a CAMECA SX50 microprobe equipped with an energy dispersive and four wavelength dispersive spectrometers at the Department of Earth and Environmental Sciences, Ludwig Maximilians University of Munich. Accelerating voltage was 15 kV and the beam current 40 nA. The beam diameter was 2 μm and the analytical software was the Xmas 4.5 from SAMx enterprise run under Windows NT. The data were reduced with the aid of the PAP algorithm.

Rock samples were analysed by OMAC Laboratories Ltd (Ireland), applying ICP Optical Emission Spectrometry. REE were analysed by Induced Neutron Activation Analysis. Detection limit for major elements is 0.01 wt %, except for TiO_2 and MnO which is 0.001 wt %. The analytical precision, calculated from replicate analyses, is better than 2 % for most major elements and better than 5 % for most trace elements and REE.

The isotopic analyses were carried out by Geospec Consultants of Edmonton, Alberta, Canada. Rock powders were weighed and totally spiked with a mixed ^{150}Nd–^{149}Sm tracer solution. Dissolution was carried out in 24N HF + 16N HNO_3 in sealed PFA Teflon® vessels at 160 °C for five days. The fluoride residue was converted to chloride with HCl, and Nd and Sm were separated by conventional cation and HDEHP-based chromatography. Chemical processing blanks were < 40 picograms of either Sm or Nd, and are insignificant relative to the amount of Sm or Nd analysed for any rock sample. The isotopic composition of Nd was determined in static mode by Multi-Collector ICP-Mass Spectrometry. All isotope ratios were normalized for variable mass fractionation to a value of $^{146}Nd/^{144}Nd = 0.7219$ using the exponential fractionation law. The $^{143}Nd/^{144}Nd$ ratio of samples is presented relative to a value of 0.511850 for the La Jolla Nd isotopic standard, monitored by use of an Alfa Nd inhouse laboratory isotopic standard for each analytical session. Sm isotopic abundances were measured in static mode by Thermal Ionization Mass Spectrometry, and are normalized for variable mass fractionation to a value of 1.17537 for $^{152}Sm/^{154}Sm$ also using the exponential law. The mixed ^{150}Nd–^{159}Sm tracer solution used was calibrated directly against the Caltech mixed Sm/Nd normal described by Wasserburg *et al.* (1981). Using this mixed tracer, the measured $^{147}Sm/^{144}Nd$ ratios for the international rock standard BCR-1 range from 0.1380 to 0.1382, suggesting a reproducibility for $^{147}Sm/^{144}Nd$ of about ± 0.1 % for real rock powders. The value of $^{147}Sm/^{144}Nd$ determined for BCR-1 is within the range of reported literature values by isotope dilution methods.

K–Ar dating was done at the Geochronology and Isotopic Geochemistry Department of Actlabs, Canada. The separate contained mainly K-feldspar with very small amounts of epidote and minor iron oxide. The K concentration was determined by Thermal Ionization Mass Spectrometry (TIMS). The argon analysis was performed using the isotope dilution procedure on a noble gas mass spectrometer in duplicate.

https://doi.org/10.1017/S0016756807003949 Published online by Cambridge University Press